MISR JOURNAL OF AGRICULTURAL ENGINEERING ISSN-Print: 1687-384X
https://mjae.journals.ekb.eg/ ISSN-Online: 2636-3062
Misr J. Ag. Eng., 39 (3): 375 - 390 **DOI:** 10.21608/mjae.2022.136171.1073

INFLUENCE OF INVERSE PULSATION ON THE CRUSHED MAIZE FLOW RATE FROM HOPPERS

Ghazy M. I.[1&*]; N. K. Ismail[2]; Z. S. Al-Ghobashy[3] and Z. E. Ismail[4]

[1] Assoc. Prof., Ag. Eng. Dept., Fac. of Ag., Mansoura U., Mansoura, Egypt.
[2] Head of Res., Ag. Bioengineering Systems Res. Dept., Ag. Eng. Res. Inst., ARC., Egypt.
[3] Grad. Stud., Ag. Eng. Dept., Fac. of Ag., Mansoura U., Mansoura, Egypt.
[4] Prof., Ag. Eng. Dept., Fac. of Ag., Mansoura U., Mansoura, Egypt.
* E-mail: mohamed_ghazy@mans.edu.eg

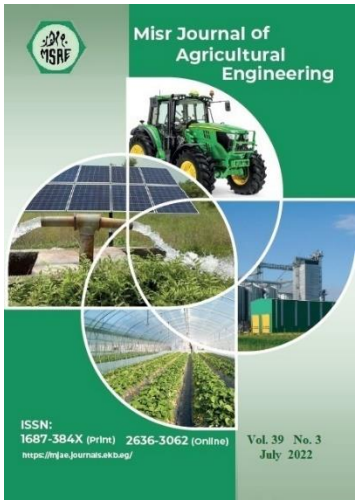

Keywords:
Funnel flow; Air chamber; Discharge efficiency; Arduino unit.

ABSTRACT

This research aims to add an inverse pulsation technique inside the hopper that speeds up the crushed grain flow and moves the stagnant fodder caused by rat-holing and arching. In the experimental lab, the hopper constructs a funnel flow system by regulating the inner inclined angle of 30° with the horizontal hopper surface. While crushed maize is discharged from the hopper, the air chamber makes a continuous cycle of constriction and expansion causing an inverse pulsation that forces the materials towards the hopper outlet. The pressure of the compressed air is controlled by a pressure gauge and the time of filling in and deflation of the air that is settled by an electronically programming code using an Arduino Uno unit. The levels of studied variables include diameter of outlet orifices "Do" (40; 45; and 50 mm), pressure of elastic air chamber "PAC" (2.0; 2.5 and 3.0 bar) per each pressure times of filling in and deflation ratio "TFD" (0.5; 0.6 and 0.7), for six batch number pulsation "NP" (1.0; 2.0; 3.0; 4.0; 5.0 and 6.0). The results cleared that the air chamber pulsation technique can improve the flow from the funnel hopper by about 51.69, 53.69 and 50.31% % at outlet orifices diameters of 40, 45 and 50 mm respectively compared to the free flow as a control unit.

1. INTRODUCTION

The increasing demands of the feeding livestock industry in Egypt have forced great accountability on the different organizations of animal feeding, improving the flow of particle material or grain out from bin/hopper “B/H”. The “B/H” is extensively used as storage facilities for solid materials in the form of granular, crusher and powder in industrial applications such as agricultural, food, chemical industry, etc. Therefore, the geometrical consideration of “B/H” discharge remains a topic of several research **(Yu and Saxén, 2011; Weinhart et al., 2016, Guo et al., 2021, Huang et al. 2022 and Zhang et al., 2022**). There are generally two dissimilar types of flow observed during “B/H” discharge, namely, mass flow and funnel flow (or central flow). The conversion from mass to funnel flow will occur for hopper angles lower than 45° (**Jenike, 1961; Ketterhagen et al., 2009, Fullard et al., 2020 and Gandia et al., 2021**). The mass flow system is described as first-in-first-out when each particle is in parallel motion and flows in an ordered manner inside the hopper, which is

analogous to the laminar flow of classical fluids (**Cheng et al., 2010; Zhang et al., 2018; Huang et al., 2020 and Tang et al., 2022**). For the funnel flow regime, described as first-in-not-necessarily-first-out, the flow is rather random and analogous to the turbulent flow of classical fluids (**Medina et al., 2014; Zhou et al., 2017 and Rabinovich et al., 2021-a).** Many advantages were found at funnel flow systems, such as: funnel flow mainly flows in the center of the hopper, which material flows faster than the material at the hopper's perimeter because the hopper angle isn't steep enough for the material to overcome the friction between the particles and the hopper wall (**Ayuga et al., 2001, Chou et al., 2002** and **Ogden and Ileleji, 2021**) produces a larger level of mixing of the particles that are in motion (**Sadowski and Rotter, 2011 and Grudzień et al., 2018),** since the material ‘‘first in” is not always ‘‘first out” due to the pocket regions **(Sielamowicz et al., 2010** and **Zaki and Siraj, 2019**), less headspace is required for the same capacity (**Ketterhagen et al., 2009**), lower pressure acting on bin walls **(Saleh** et al., **2018)** and the walls are subject to less abrasion (**Rycroft et al., 2006**).

Depending on the material, a funnel-flow hopper can be subject to numerous common flow problems, involving segregation (separation by size), bridging (cohesive arch of material over the hopper's discharge), rat-holing, and flooding (**Liu et al., 2019 and Huang et al., 2020**). The main one of funnel flow disadvantages is that forming a pocket that resists the material flows out and remains constant until emptying at the end of the bin emptying (**Maynard, 2004; Ketterhagen et al., 2009 and Rabinovich et al., 2021-b).**

It is important to prevent or solve this problem; one of them is to use flow correcting inserts. These inserts are added to “B/H” which grains (or a portion of the grains) flow through or around them, that used to convert a funnel flow into the mass flow regime (**Wójcik, et al., 2012; Haertl et al., 2008; Kobyłka et al. 2019 and Sun et al., 2020).** Another attempt, adding a large double cone which use to reduce the degree of funnel flow, and in the case of the large double cone, the “B/H” may be operating in the mass flow regime **(Fullard et al., 2020).** In summary, reducing wall roughness and presenting an insert into the “B/H” reduces the adventive mixing, reduces the size of the stagnant pocket zone, and transitions the “B/H” closer to, or fully into, the mass flow regime**. Wassgren (2002), Zhang et al. (2018) and Pascot et al. (2022)** used a vertical vibration as a parameter affecting hopper flow material and compared it with horizontal vibration.

To solve these problems, it is necessary to systematically understand the discharge physiognomies, especially the influence mechanism of geometric strictures and particle specifications on the discharge characteristics.

- So, the focus of this paper is to investigate a new technique that uses an elastic air chamber adept as inverse pulsation controlling granular flow rate.
- Utilization of Arduino circuit to control the variable parameters.

2. MATERIALS AND METHODS

General description of the installation

Tests were conducted in Agric. Eng. Dept., Fac. of Agric., Mansoura Univ., from 2019 to 2021. The bin/hopper “B/H” was fabricated in a special workshop at Mit Badr Khames, Dakahlia Governorate. The proposed design unit is a combined unit of a cylindrical bin, a

compressor, an elastic air chamber, electronic circuit, Arduino Uno board, and a computer as illustrated in figures (1 and 2).

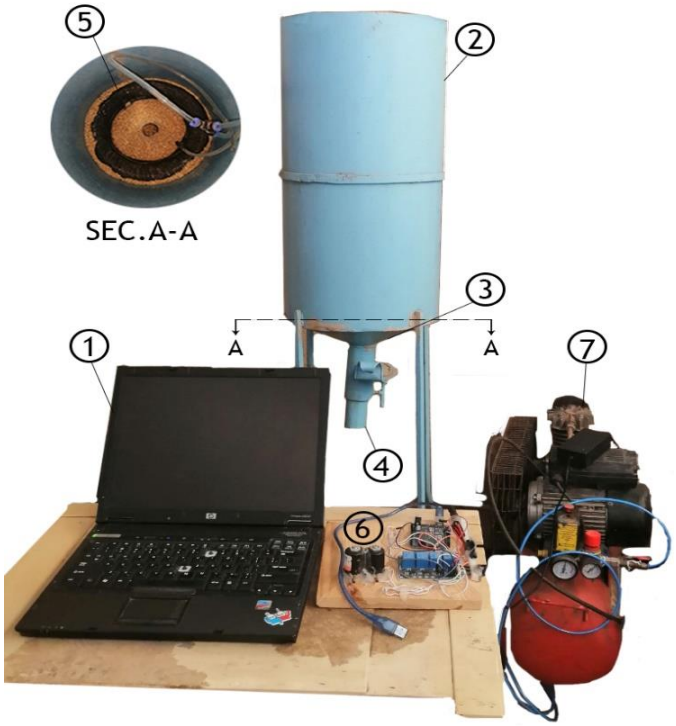

1-Computer, 2- Bin, 3- Hopper, 4- Orifice, 5- Air chamber, 6- Electronic circuit and 7- Air compressor

Fig. (1): The experimental station for evaluation "B/H performances

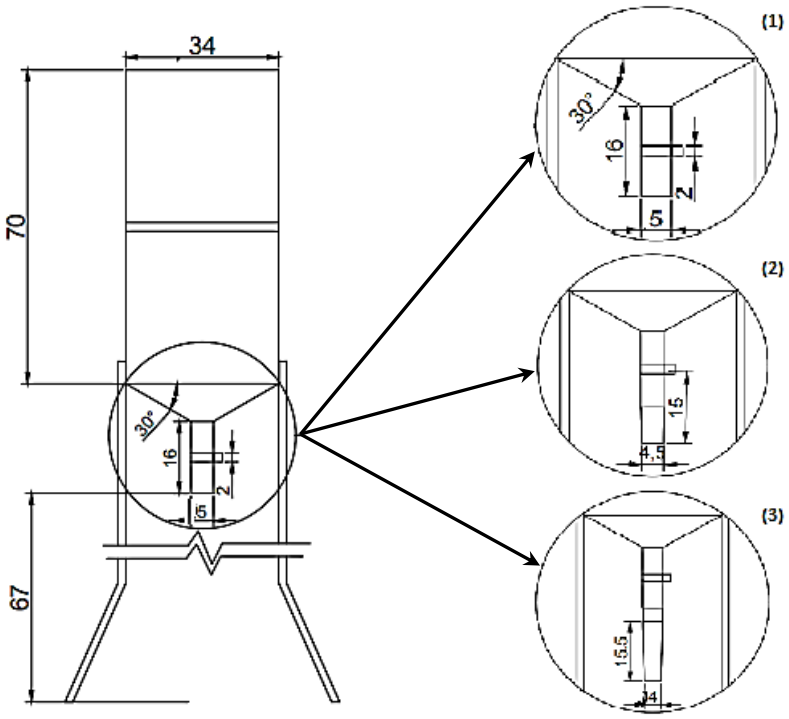

1- at "Do" of 50 mm 2- at "Do" of 45 mm 3- at "Do" of 40 mm

Fig. (2): Layout of experimental bin/hopper with different orifices diameters "Do"

The bin/hopper "B/H"

It is made of an iron sheet of 2.0 mm thickness with a total height of ≈1730 mm from the ground surface and 340 mm diameter. It is a combination of a cylindrical bin of 700 mm height and a conical hopper of 150 mm height and with different diameters of outlet orifices "Do" as shown in figure (2). The bin has four stands for support. Each stand has a height of 880 mm from the surface of ground. The conical hopper was designed to serve a funnel flow regime by an inclined angle of 30° to the horizontal plane.

Air compressor

Air compressor of 1.0 HP and tank of 25 L "model APT SG1051" are used and the gas pressure was controlled by a gauge unit.

Elastic air chamber

The air chamber is a pneumatic inner tube tire made from rubber with 200 mm inner diameter and an 400 mm outer diameter under airless condition, as shown in figure (3). The elastic air chamber is set at the bottom of the bin and directly above the cone hopper. The pneumatic air tube "PU" and plastic pneumatic tube connectors (fittings PE T-type) for pushing in Tee 3-Way used to supply the compressed air to the bin/hopper (figures (4-A) and (4-B)).

Fig. (3): The air chamber

A- air tube "PU" B- Tee 3-way

Fig. (4): The connected elements with the unit air supply

The electronic circuit

It is mainly constructed from Arduino-UNO board, located on an Atmel 8-bit AVR microcontroller, running by a 16 MHz crystal oscillator (figures 5 and 6). The board contains a 5V regulator, many peripheral parts, and a microcontroller with a self-programming pre-loaded code. For the Arduino-UNO boards, a USB interface is available through an RS232-USB converter that is located on the board. From the total of 20 i/o pins, 6 of them may be used for analog input as digital i/o. Another 6 pins can generate pulse-width-modulated (PWM) output as digital i/o. PWM outputs may be converted to analog output by filtering the pulses with an RC filter. Also it contains two relays. It is an electrically operated switch which is used to close and open the circuit electronically and electromechanically. Three TONGLING relay with specification of "10A-250V-AC", "15A-125V-AC" and "10A -250V-AC" model (JQC-3FF-S-Z) were used. To stop/ start and control the air flow, a pneumatic valve of "2L5" with specification of "VZ-2.2"- DC 24V- 0-0.6MPA" is used.

Computer

The computer is windows 7 HP laptop used only for coding the Arduino Uno board with a program version 1.8.3.

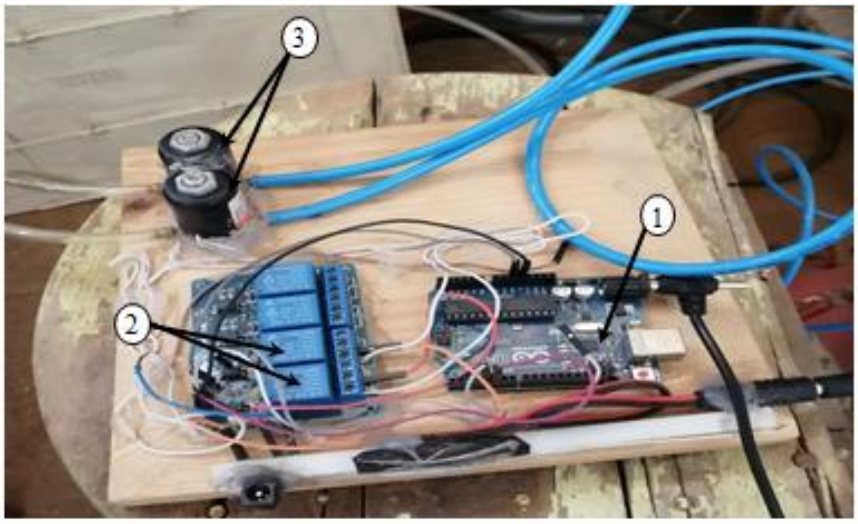

1- Arduino-UNO board 2- Relays 3- Pneumatic valves

Fig. (5): The electronic circuit

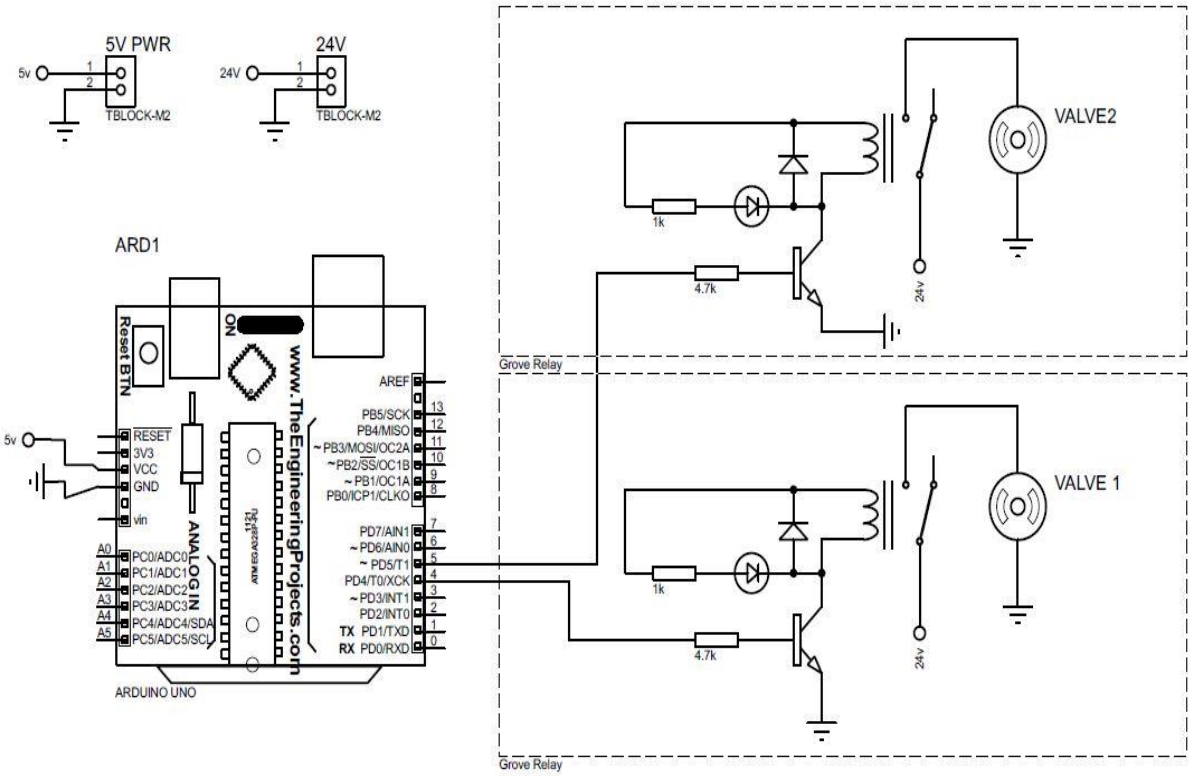

Fig. (6): Arduino-UNO cycle

Inverse pulsation technique

The proposed design depends on placing a flexible unit “elastic air chamber” in the perturbation zone of the fodder flow to overcome the main problem that faces the funnel flow rate of the bin/hopper “B/H” system. This unit sends air pulses as volumetric waves "inversely pulsations" towards the fodder. These waves were done using the electrical system that was provided to operate a compressor and an electronic circuit. It is used to control the time of in/out air which uses to inflate and deflate an elastic air chamber. This investigation may help to move the stagnant fodder caused by rat-holing and arching. Consequently, it may improve the fodder flow from the exit orifice.

The experimental procedure and study variables

Pre experiments were carried out to determine the crushed maize properties, moisture content, bulk density, porosity, angle of repose, coefficient of friction and particle size distribution using common methods according to **Ismail and Hemeda (1991) and Fawal et al. (2008).** The study was conducted in Ismail's Lab (2004) at Ag. Eng. Dept. of Mansour U. By filling the hopper with 30 kg of crushed maize, then the electronic circuit work. The amount of discharge at 6 sections were determined through the time for each section. All treatments were adapted under three diameters of outlet orifices "Do" (40; 45; and 50 mm) and three pressures on elastic air chamber "PAC" (2.0; 2.5 and 3.0 bar) under each pressure there were three different times of filling/in and deflation "TFD" (5/10, 10/20, and 15/25) at "PAC" of 2.0 bar; (2/4, 4/6 and 6/12) at "PAC" of 2.5bar and (0.5/3.0, 1.0/6.0 and 1.5/9.0S) at "PAC" of 3.0 bar. All treatments were conducted at six batches number pulsation "NP" (1.0; 2.0; 3.0; 4.0; 5.0 and 6.0). All experiments were evaluated by identifying the operating time "OPT, s"; discharge "D, $kg.s^{-1}$" and discharge efficiency, "De, %". The experiments were done under two groups, the free flow as control treatment then by the investigated device.

The Moisture content (MC, %) was determined using the electric blast drying oven and adjusted to $103^{\pm 1}$ ◦C for 3–4 h (**Tang et al., 2021**). The wet basis representation was applied as follows:

$$\mathrm{MC} = \frac{(\mathrm{WW}-\mathrm{DW})}{\mathrm{WW}} \times 100 \ \%$$

Where: WW = Wet mass of the sample (g) and DW = Dry mass of the sample (g)

The bulk density was determined using the common methods (Matouk, et al., 2004 and Ismail and Hemeda, 1991).

The particle size distribution was evaluated using an apparatus consisting of six different sieves mesh mounted on each other and installed on a frame. The samples of crushed maize were taken from five various levels. After sieving all the individual fractions, they were weighed and converted to a percentage of the total sample mass (Ismail, et al., 2017).

Statistical analyzing and mathematical model, a factorial experiment according to randomized complete blocks design of samples layout design was taken. Then the multiple regression analysis of the operating time is used by Excel version 10 to produce the mathematical model.

3. RESULTS AND DISCUSSION

Some physical and mechanical properties of crunching maize

The properties of crushed maize material were presented in the table (1). From the table, it can be clear that the average moisture content, bulk density, angle of repose and coefficient of friction on the metal plate were 10.38%, 0.5992 $g.cm^{-3}$, 50°, and 1.245 respectively for crunching maize.

Table (1): Physical and mechanical properties of crunched maize

Index	Moisture content, %	Bulk density, $g.cm^{-3}$	Porosity, %	Angle of repose, degree	Coefficient of friction
Crushed maize	$10.38^{\pm 0.37}$	$0.5992^{\pm 0.006}$	58.1	50.0	$1.245^{\pm 1.097}$

The percentage of crunching maize particle size distribution

The percentage of crunching maize particle size distribution as shown in figure (5) showed that the highest percentage of the crunching maize particle size distribution 35.31% at sieve holes diameter of 2-3 mm. The figure also illustrated that the high percentages of crunching maize particle size distribution were about 82.65% at the sieve holes diameters ranging from 1 to 4 mm. The best-fit equation of the crunching maize particle size distribution is the polynomial equation. It achieves the coefficient of determination (R^2) about 0.943.

$$PSD, \% = 0.5897SHD^4 - 6.7744\ SHD^3 + 20.097\ SHD^2 - 4.0824\ SHD \qquad R^2 = 0.943$$

Where:

PSD = Particle size distribution, %

SHD = Sieve holes diameter, mm

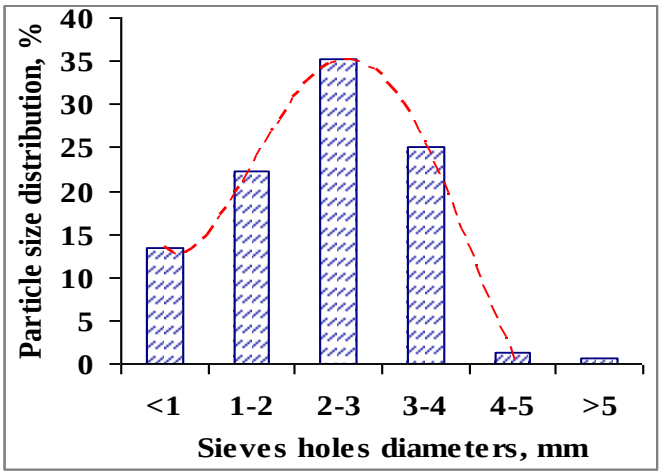

Fig. (5): The percentage of crunching maize particle size distribution

Free flow of crushing maize "control"

The free flow of crushing maize before modification is tabulated in Table (2) using orifice diameters "Do" of 40, 45 and 50 mm. The data from the table indicated that the operating time "OPT,s" was decreased by 5.94, 5.68 and 5.27 sec respectively. These may be due to the crushed grain making a rat-holing or arched form. Also, it can show that both discharge "D, $kg.s^{-1}$" and discharge efficiency "De, %" have a distribution nearly to normal distribution curve. That accomplished the highest values using the 45 mm orifice diameter. These results may be due to at this diameter the suitable flow and repose angles and the geometric parameters of the bin were established. The decrease in the flow material efficiency requires more modification of the B/H system.

Table (2): The description of crushing maize free flow from hopper

"Do", mm	"OPT", s	"D", $kg.s^{-1}$	"De", %
40	5.94	1.0149	33.83
45	5.68	1.025475	34.18
50	5.27	0.95991	31.99

The evaluation parameters

To judge the use of the inverse pulsation on the flow out of crushed corn from the hopper the following evaluations was conducted. Figure (6) illustrated the effect of batch number

pulsation on discharge "D, kg.s^{-1}" and discharge efficiency "De", % at different orifice diameters and air pressure of 2.0 bar.

Figure (6-A) showed that by increasing the batch number pulsation from 1 to 6 the accumulative crushing maize discharge "D, kg.s^{-1}" increased from 1.932 to 2.188, from 2.05 to 2.35 and from 1.75 to 2.01 kg.s^{-1} at orifice diameters of 40, 45 and 50 mm, respectively. This result cleared that the discharge using the orifice diameters of 45 mm is the highest of flow out. Meanwhile, figure (6-B) illustrated the discharge efficiency "De %" of crushing maize which had the same trend of discharge. It cleared that with the increase of batch number pulsation from 1 to 6 the discharge efficiency increased from 64.40 to 72.93, 65.61 to 75.33 and 58.17 to 66.97 % respectively at orifice diameters of 40, 45 and 50 mm. Generally, at air pressure 2.0 bar the highest discharge and discharge efficiencies were 2.35 kg.s^{-1} and 75.33% respectively at an orifice diameter of 50 mm.

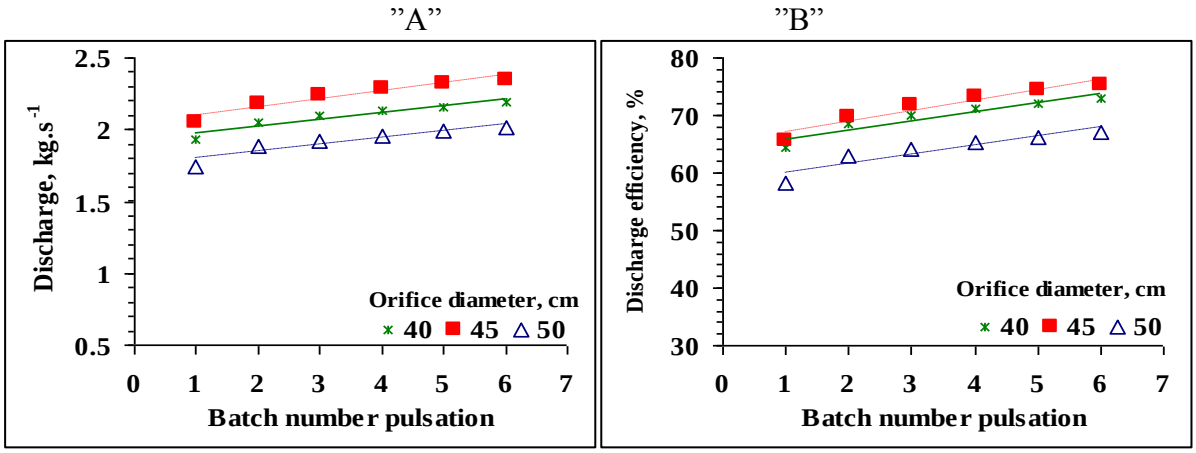

Fig. 6: Bach number pulsation via valuation parameters at an air pressure of 2.0 bar

Figure (7) demonstrated the effect of batch number pulsation on discharge (figure 7-A) and discharge efficiency (figure 7-B) at different orifice diameters and air pressure of 2.5 bar. The figure showed that the highest discharge was 2.17 kg.s^{-1} and discharge efficiency was 72.28% were found at the same previous variables level using the air pressure 2.0 bar. On the other side, the lowest data found at batch number pulsation of 1.0 for the discharge and discharge efficiency were 1.60 kg.s^{-1}and 59.86% by using orifice diameter of 50 mm respectively.

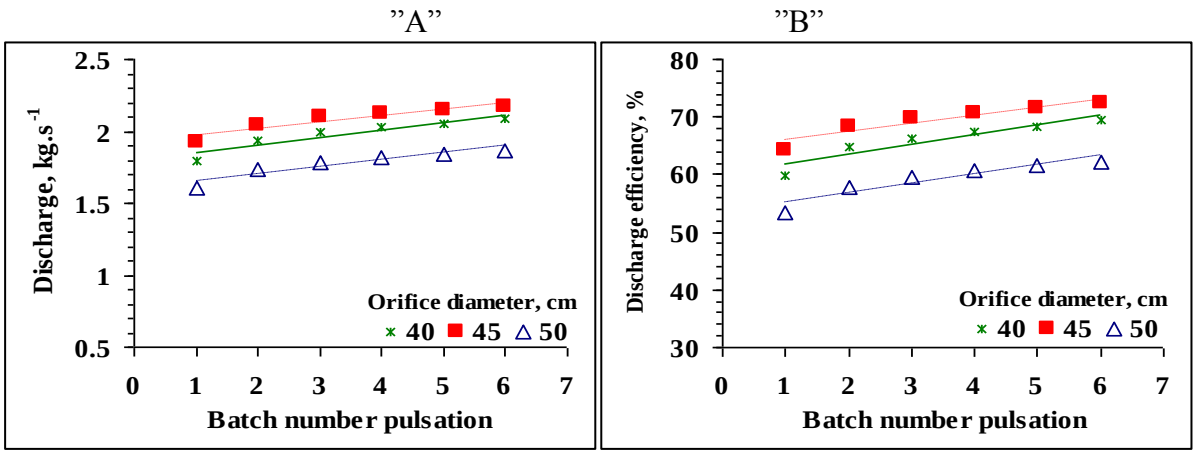

Fig. 7: Bach number pulsation via valuation parameters at an air pressure of 2.5 bar

Figure (8) illustrated the effect of batch number pulsation on discharge (figure (8-A) and discharge efficiency (figure 8-B) at different orifice diameters and air pressure of 3.0 bar. The figure cleared that by increasing the batch number pulsation from 1 to 6 times, the crushing maize discharge and discharge efficiency increased from 1.77 to 2.03 kg.s^{-1} and 59.08 to 67.58 % at an orifice diameter of 40 mm. Also, with an orifice diameter of 45mm the crushing maize discharge and discharge efficiency increased from 1.89 to 2.12 kg.s^{-1} and from 62.97 to 70.80 % by increasing the batch number pulsation from 1 to 6. Hence, using an orifice diameter of 50 mm, the discharge and discharge's efficiency were increased from 1.67 to 1.92 kg.s^{-1} and 55.66 to 63.96 %.

By increasing the pressure inside the air chamber from 2.0 to 2.5 bar, the rate of material out increased by about 1.13 times. But by increasing the pressure from 2.5 to 3.0 bar, it was decreased by about 0.95 times. It may be due to increasing the air chamber pressure from 2.5 to 3.0 bar that reduce the size bottom of the feeding flow and consequently, the suffocation of the flow from the tank.

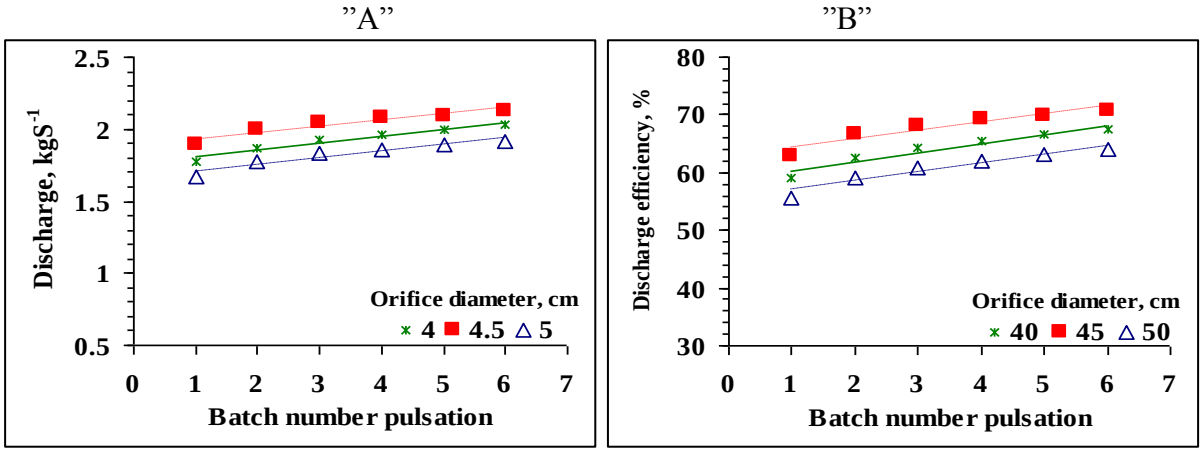

Fig. 8: Bach number pulsation via valuation parameters at an air pressure of 3.0 bar

The inflate and deflate an elastic air chamber ratio "TED"

The operation time

The multiple regression equation of operating time "OPT" via orifice diameters" Do, mm", air pressure "APC, bar", rate of "TFD" and batch number pulsation "Np" had a significant effect on the coefficient of determination of R^2=0.8249 (Fig. 9).

$$OPT = -8.05 + 4.28\ \text{"Do"} - 1.76APC - 0.66TFD + 1.99NP \qquad (R^2 = 0.8249)$$

The discharge rate

Figure (10-A) shows that the highest discharge of 2.37 kg.s^{-1} can be obtained at "Do" of 45mm and TFD1-2 (on/off ratio 10 to 20) with two cycles per mint and 2.0 bar air pressure in the air chamber. Increasing the pressure in the air chamber to 2.5bar (figure 10-B), the highest discharge was 2.25 kg.s^{-1} was found at" Do" of 4 0mm with TFD2-1(on/off ratio 2 to 4) with 10 cycles/ min. During increasing air chamber pressure to 3.0 bar (figure 10-C), the 2.18 kg.s^{-1} flow discharge recorded the height values were found at TFD3-2 (on/off ratio 1 to 6) with 8.25 cycles/min and "Do" of 45mm. While the minimum discharge of 1.82 kg.s^{-1} can be obtained at "Do" of 50 mm and TFD1-2 (on/off ratio 10 to 20) with two cycles per mint and 2.0 bar air pressure in the air chamber as shown in figure (10-A). By increasing the pressure

in the air chamber to 2.5bar (figure 10-B), the lowest discharge was 1.86 kg.s^{-1} was found at "Do" of 50 mm with TFD2-2 (on/off ratio 4 to 6) with 6 cycles/ min. During increasing air chamber pressure to 3.0 bar (figure 10-C), the 1.90 kg.s^{-1} flow discharge recorded the lowest value was found at TFD3-1 (on/off ratio 5 to 3) with 7.5 cycle/ min and "Do" of 50mm.

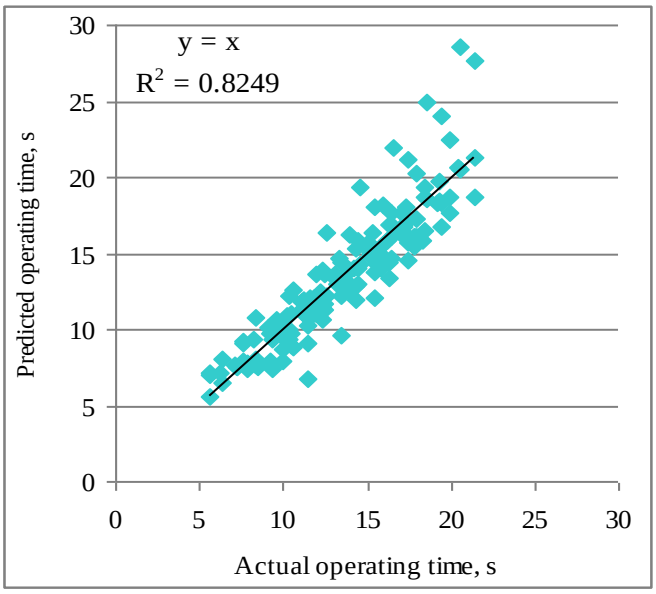

Fig. 9: The predicted via the actual operating time

The discharge efficiency

Figure (11-A) showed that the discharge efficiency of 78.85% can be obtained at Do of 45mm and TFD1-2 (on/off ratio 10 to 20) with two-cycle/mint and 2.0 bar air pressure in the air chamber. By increasing the pressure in the air chamber to 2.5bar (figure 11-B), the highest discharge efficiency was 75.05% found at "Do" of 40mm with TFD2-1 (on/off ratio 2 to 4) with 10 cycles per min. During increasing air chamber pressure to 3.0 bar (figure 11-C), the 72.78% flow discharge efficiency recorded the height value was found at TFD3-2 (on/off ratio 1 to 6) with 8.52 cycles/min and "Do" of 45mm.

While the minimum discharge efficiency of 60.68% can be obtained at "Do" of 50 mm and TFD1-2 (on/off ratio 10 to 20) with two-cycle per mint and 2.0 bar air pressure in the air chamber as shown in figure (11-A). Increasing the pressure in the air chamber to 2.5bar (figure 11-B), the lowest discharge efficiency was 62.06% found at "Do" of 50 mm with TFD2-2 (on/off ratio 4 to 6) with 6 cycles/ min. During increasing air chamber pressure to 3.0 bar (figure 11-C), the 63.38% flow discharge efficiency recorded the lowest value was found at TFD3-1(on/off ratio 5 to 3) with 7.5 cycles/ min and "Do" of 50 mm.

This variation of crushed maize discharge "D, kg.s^{-1}" or discharge efficiency may be due to the interaction between the number of systole and diastole time with the expansion or contraction of the air chamber and the opening of the material exit from the tank. It is mainly regarding the interaction among internal friction, surface out frictions and the hopper's inner inclined angle with the horizontal hopper surface. Also, it is regarding to the random interaction between variables where there is no definite trend of correlation between them.

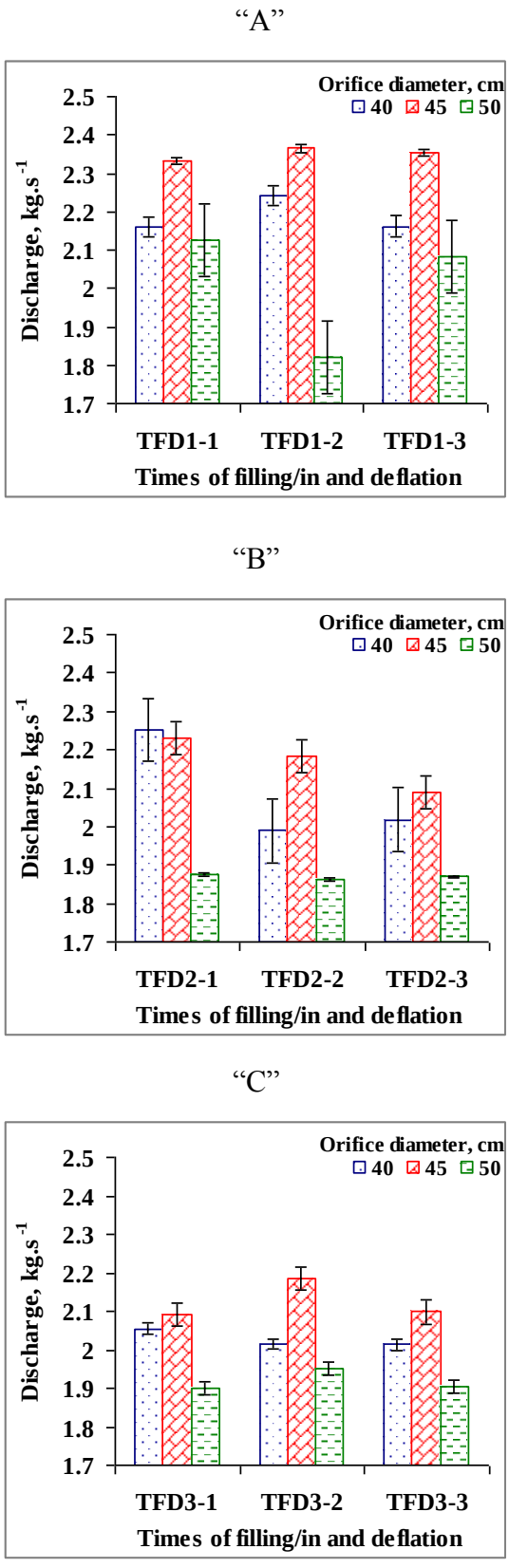

Figure (10): The discharge as affected by the systole and diastole of air chamber ratio

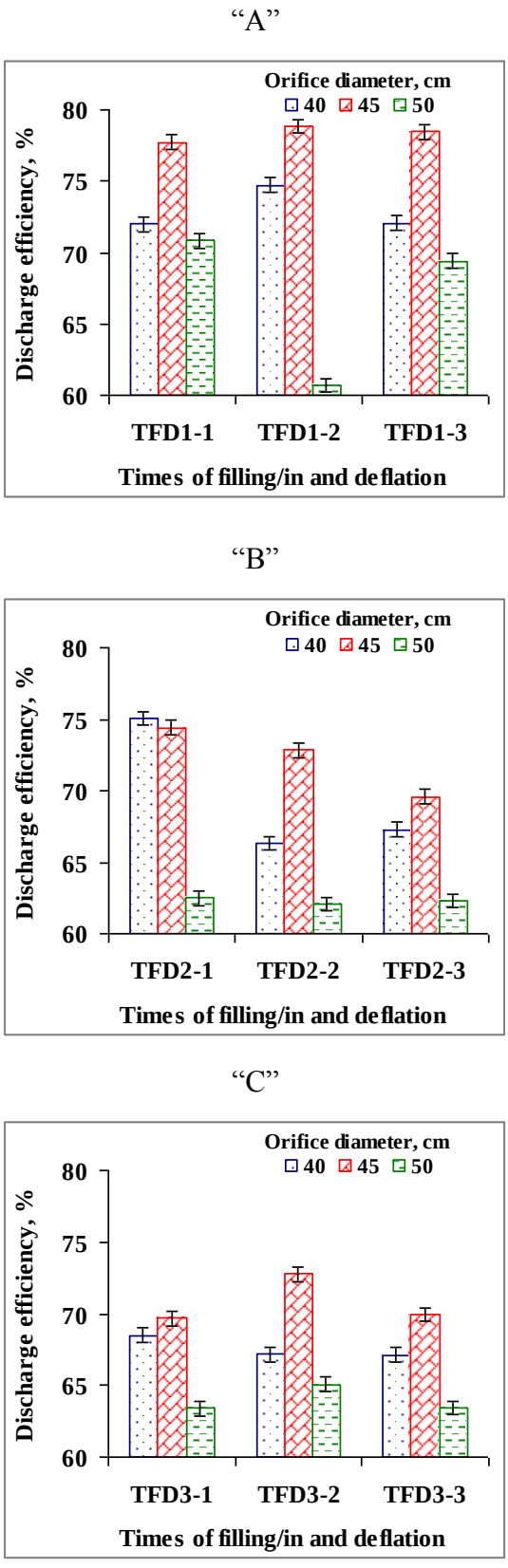

Figure (11): The discharge efficiency as affected by the systole and diastole of air chamber ratio

The conventional and developed system evaluation

Regarding the control data in table (2) and the data in figure 11 "after applying the inverse pulsation technique", the results cleared that, the air chamber pulsation technique can improve the flow from the funnel hopper by about 51.69, 53.69 and 50.31% respectively at outlet orifice diameters of 40, 45 and 50 mm compared to the free flow which stopped flow after 5.63 sec.

4. CONCLUSIONS

The air chamber pulsation technique can improve the flow from the funnel hopper by about 51.69, 53.69 and 50.31% respectively at outlet orifice diameters of 40, 45 and 50 mm compared to the free flow which stopped flow after 5.63 sec. Also, the results cleared that the highest discharge efficiencies obtained was 75.05%; using an orifice diameter of 40 mm, air pressure 2.5 bar and air in/out the time of 6.0/12.0 S; 78.85%; using an orifice diameter of 45 mm, air pressure 2.0 bar and air in/out the time of 10.0/20.0 S; and 70.84%; using orifice diameter of 50 mm, air pressure 2.0 bar and air in/off the time of 5.0/10.0 sec.

5. REFRENCES

Ayuga, F.; M. Guaita and P. Aguado (2001). Discharge and the eccentricity of the hopper influence on the silo wall pressures. J. Eng. Mech., 127, 1067 - 1074.

Cheng, Y.M.; K.T. Chau; L.J. Xiao and N. Li (2010). Flow pattern for a silo with two layers of materials with single or double openings. J. Geotech. Geoenvironmental Eng., 136, 1278 - 1286.

Chou, C.S.; J.Y. Hsu and Y.D. Lau (2002). The granular flow in a two-dimensional flat-bottomed hopper with eccentric discharge. Phys. A Stat. Mech. Appl., 308, 46 - 58.

Fawal, Y.A.; N.K. Ismail and E.H. Mousa (2008). Some physical and engineering properties of sugar beet seeds in relation with some agricultural mechanical. J. Agric Sci. Mansoura Univ., 33(1): 273-282.

Fullard, L.A.; A.J.R. Godfrey; M.F. Manaf; C.E. Davies; A. Cliff and M. Fukuoka (2020). Mixing experiments in 3D-printed silos; the role of wall friction and flow correcting inserts. Advanced Powder Technology, 31, 1915 - 1923.

Gandia, R.M.; E.A.D.O. Júnior; F.C. Gomes; W.C.D. Paula and K.C. Dornelas (2021). Experimental pressures exerted by maize in slender cylindrical silo: Comparison with Iso 11697. Engenharia Agrícola, 41 (6): 576 - 590.

Grudzień, K.; Z. Chaniecki and L. Babout (2018). Study of granular flow in silo based on electrical capacitance tomography and optical imaging. Flow Meas., Instrum, 62, 186 - 195.

Guo, C.; M. Ya; Y. Xu and J. Zheng (2021). Comparison on discharge characteristics of conical and hyperbolic hoppers based on finite element method. Powder Technology, 394, 300 - 311.

Haertl, J.; J. Ooi; J. Rotter; M. Wojcik; S. Ding and G.G. Enstad (2008). The influence of a cone-in-cone insert on flow pattern and wall pressure in a full-scale silo. Chem. Eng. Res. Des., 86 (4): 370 – 378.

Huang, X.; Q. Zheng; A. Yu and W. Yan (2020). Shape optimization of conical hoppers to increase mass discharging rate. Powder Technology, 361, 179 – 189.

Huang, X.; Q. Zheng; A. Yu and W. Yan (2022). A design method of hopper shape optimization with improved mass flow pattern and reduced particle segregation. Chemical Engineering Science, 253, 1 – 15.

Ismail, N. K.; O. A. Fouda; M. C. Ahmad and M. M. Mousa (2017). Influence of knives wear phenomena on hammer mill productivity and product quality. J. Soil Sci. and Agric. Eng., Mansoura Univ., Vol. 8 (7): 347 - 353.

Ismail, Z.E. (2004). The first report of project "Developing the metering unit of the pneumatic planter'. 1- The factors affecting seed-metering unite performance. J. Agric. Sci. Mansoura Univ. 33(9): 6511 – 6525.

Ismail, Z.E. and M.A. Hemeda (1992). Expected profile shape of corn furrow ridge as affected by the operation condition. Misr. J. Ag., 9(3): 450 – 462.

Jenike, A.W. (1961). Gravity flow of bulk solids. University of Utah, Salt Lake City. 52 (29): pp. 1– 309.

Ketterhagen, W.R.; J.S. Curtis; C.R. Wassgren and B.C. Hancock (2009). Predicting the flow mode from hoppers using the discret.e element method. Powder Technology, 195, 1 – 10.

Kobyłka, R.; M. Molenda and J. Horabik (2019). Loads on grain silo insert discs, cones, and cylinders: Experiment and DEM analysis. Powder Technology, 343, 521 – 532.

Liu, H.; F. Jia; Y. Xiao; Y. Han; G. Li; A. Li and S. Bai (2019). Numerical analysis of the effect of the contraction rate of the curved hopper on flow characteristics of the silo discharge. Powder Technology, 356, 858 – 870.

Matouk, A.M.; S.M. Radwan; M.M. El-Kholy and T.R. Ewies (2004). Determination of grains density and porosity for some cereal crops. Misr J. Agric. Eng. 21 (3): 623 – 641.

Maynard, E.P. (2004). Practical solutions for solving bulk solids flow problems. IEEE-IAS/PCA Cement Industry Technical Conference, 139 – 147.

Medina, A.; D. Cabrera; A. López-Villa and M. Pliego (2014). Discharge rates of dry granular material from bins with lateral exit holes. Powder Technology, 253, 270 – 275.

Ogden, C.A. and K.E. Ilelej (2021). Physical characteristics of ground switchgrass related to bulk solids flow. Powder Technology, 385, 386 – 395.

Pascot, A.; J.Y. Morel; S. Antonyuk;, M. Jenny , Y. Cheny and S.K. De Richter (2022). ischarge of vibrated granular silo: A grain scale approach. Powder Technology, 397, 1-11.

Rabinovich, E.; H. Kalman and P.F. Peterson (2021-a). Granular material flow regime map for planar silos and hoppers. Powder Technology, 377, 597 – 606.

Rabinovich, E.; H. Kalman and P.F. Peterson (2021-b). Parametric study and design procedure for planar silos and hoppers. Powder Technology, 388, 333 – 342.

Rycroft, C.H.; G.S. Grest and J.W. Landry (2006). Analysis of granular flow in a pebble-bed nuclear reactor. Phys. Rev. E 74, 1-16.

Sadowski, A.J. and J.M. Rotter (2011). Buckling of very slender met.al silos under eccentric discharge. Eng. Struct., 33, 1187–1194.

Saleh, K.; S. Golshan and R. Zarghami (2018). A review on gravity flow of free-flowing granular solids in silos – basics and practical aspects. Chem. Eng. Sci., 192, 1011 – 1035.

Sielamowicz, I.; M. Czech and T.A. Kowalewski (2010). Empirical description of flow parameters in eccentric flow inside a silo model. Powder Technology, 198, 381 – 394.

Sun, D.; H. Lu; J. Cao; Y. Wu; X. Guo and X. Gong (2020). Flow mechanisms and solid flow rate prediction of powders discharged from hoppers with an insert. Powder Technology, 367, 277 – 284.

Tang, H.; C. Xu; Y. Jiang; J. Wang; Z. Wang and L. Tian (2021). Evaluation of physical characteristics of typical maize seeds in a cold area of north china based on principal component analysis. Processes, 9, 1 – 16.

Tang, J.; H. Lu; X. Guo and H. Liu (2022). Discharge characteristics of non-gravity-driven powder in horizontal silos. Powder Technology, 400, 1-9.

Wassgren, C. R. (2002). Effects of vertical vibration on hopper flows of granular material. Physics of Fluids. 14 (10): 3439–3448.

Weinhart, T.; C. Labra; S. Luding and J.Y. Ooi (2016). Influence of coarse-graining parameters on the analysis of DEM simulations of silo flow. Powder Technology, 293, 138 – 148.

Wójcik, M.; J. Tejchman and G.G. Enstad (2012). Confined granular flow in silos with inserts-full-scale experiments. Powder Technology. 222, 15 – 36.

Yu, Y. and H. Saxén (2011). Discrete element method simulation of properties of a 3D conical hopper with mono-sized spheres. Adv. Powder Technology, 22, 324 – 331.

Zaki, M. and M.S. Siraj (2019). Study of a flat-bottomed cylindrical silo with different orifice shapes. Powder Technology, 354, 641 – 652.

Zhang, C.; C. Qiu; C. Pu; X. Fan and P. Cao (2018). The mechanism of vibrations-aided gravitational flow with overhanging style in hopper. Powder Technology, 327, 291 – 302.

Zhang, D.; S. Dong; H. Guo; X. Yang; L. Cui and X. Liu (2022). Flow behavior of granular material during funnel and mixed flow discharges: A comparative analysis. Powder Technology, 396, 127-138.

Zhou, Y.; P. Y. Lagrée; S. Popinet; P. Ruyer and P. Aussillous (2017). Experiments on, and discrete and continuum simulations of, the discharge of granular media from silos with a lateral orifice. J. Fluid Mech. 829, 459 – 485.

تأثير النبض العكسي على معدل تدفق مجروش حبوب الذرة من الخزانات

د. محمد إبراهيم غازى[١]، أ.د. ناهد خيري إسماعيل[٢]، م. زينب سليمان الغباشى[٣] و أ.د. زكريا إبراهيم إسماعيل[٤]

[١] أستاذ مساعد بقسم الهندسة الزراعية - كلية الزراعة - جامعة المنصورة - مصر.

[٢] رئيس بحوث بقسم بحوث نظم الهندسة الحيوية الزراعية - معهد بحوث الهندسة الزراعية - مركز البحوث الزراعية - مصر.

[٣] طالبة دراسات عليا بقسم الهندسة الزراعية - كلية الزراعة - جامعة المنصورة - مصر.

[٤] أستاذ بقسم الهندسة الزراعية - كلية الزراعة - جامعة المنصورة - مصر.

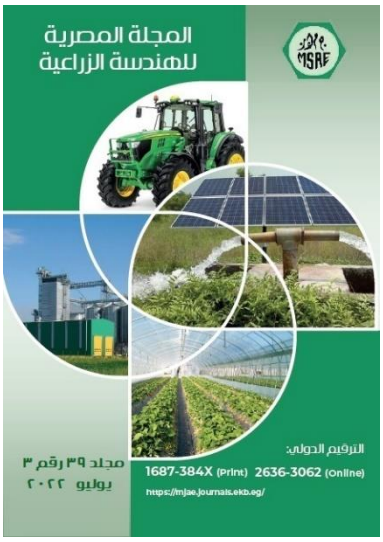

الكلمات المفتاحية:
السريان المضطرب؛ غرفة الهواء؛ كفاءة التصرف؛ النبض العكسي للحركة.

الملخص العربى

من أهم المشكلات التي تواجه حركة الحبوب والأعلاف داخل الخزانات بطء التصرف وتوقفه الناتج عن عدم إضافة وسيلة لخلخلة الحبوب والأعلاف داخل أو خارج الخزان خاصة في حالة تطبيق نظام السريان النفقي. لذا يهدف هذا البحث إلى إضافة وسيلة داخل الخزانات تعمل على سرعة تدفق الحبوب أو الأعلاف. ولتحقيق هذا الهدف تم تصميم قادوس بنظام السريان النفقي ذو زاوية ميل مع السطح الأفقي للخزان ٣٠°. وتم إضافة إطار هوائي مرن في نهاية الخزان وأعلى القادوس. يتم ملء الإطار الهوائي المرن وتفريغه من الهواء في دورات مستمرة من الانقباض والتمدد مما يتسبب في نبضة عكسية تجبر المواد على التحرك نحو مخرج القادوس. وقد تمت التجارب على مجروش ذرة (متوسط أقطاره ١-٤ مم). وخلال التجارب تم التحكم في ضغط الهواء المضغوط بواسطة مقياس ضغط. كما يتم التحكم في وقت ملء وتفريغ الهواء بواسطة ضبط الكود الإلكتروني باستخدام وحدة(Arduino Uno). وقد اشتملت مستويات المتغيرات المدروسة على: قطر فتحات الخروج (٤٠، ٤٥ و٥٠ مم)؛ الضغط داخل إلى غرفة الهواء المطاطية (٢,٠، ٢,٥ و٣,٠ بار)، ونسب أوقات الملء والتفريغ (٠,٥، ٠,٦ و٠,٧) وذلك عند عدد ست دورات نبضيه (١,٠، ٢,٠، ٣,٠، ٤,٠، ٥,٠ و٦,٠). أوضحت النتائج أن أعلى كفاءة تصرف تم الحصول عليها كانت ٧٥,٠٥٪. باستخدام فتحة قطرها ٤٠ مم، وضغط الهواء ٢,٥ بار، ووقت دخول/خروج الهواء ١٢,٠/٦,٠ ثانية؛ ٧٨,٨٥٪ ؛ باستخدام فتحة قطرها ٤٥ مم، وضغط الهواء ٢,٠ بار، ووقت دخول/خروج الهواء ٢٠,٠/١٠,٠ ثانية؛ ٧٠,٨٤٪ ؛ باستخدام فتحة قطرها ٥٠ مم، وضغط الهواء ٢,٠ بار، ووقت دخول/خروج الهواء ١٠,٠/٥,٠ ثانية.